Surprises in the suddenly-expanded infinite well

2008 J. Phys. A: Math. Theor. 41 075301

(http://iopscience.iop.org/1751-8121/41/7/075301)

J. Phys. A: Math. Theor. **41** (2008) 075301 (23pp) doi:10.1088/1751-8113/41/7/075301

Surprises in the suddenly-expanded infinite well

Claude Aslangul

Laboratoire de Physique Théorique de la Matière Condensée, Laboratoire associé au CNRS (UMR 7600), Université Paris 6, 2 place Jussieu, 75252 Paris Cedex 05, France

E-mail: aslangul@lptmc.jussieu.fr

Received 7 September 2007, in final form 12 December 2007
Published 5 February 2008
Online at stacks.iop.org/JPhysA/41/075301

Abstract

I study the time evolution of a particle prepared in the ground state of an infinite well after the latter is suddenly expanded. It turns out that the probability density $|\Psi(x,t)|^2$ shows up quite a surprising behaviour: for definite times, *plateaux* appear for which $|\Psi(x,t)|^2$ is constant on finite intervals for x. Elements of theoretical explanation are given by analysing the singular component of the second derivative $\partial_{xx}\Psi(x,t)$. Analytical closed expressions are obtained for some specific times, which easily allow us to show that, at these times, the density organizes itself into regular patterns provided the size of the box is large enough; more, above some critical size depending on the specific time, the density patterns are independent of the expansion parameter. It is seen how the density at these times simply results from a construction game with definite rules acting on the pieces of the initial density.

PACS numbers: 03.65.−w, 03.65.Ge, 85.35.Be

(Some figures in this article are in colour only in the electronic version)

1. Introduction

This paper is devoted to some strange dynamical aspects around a problem which is often presented as the simplest one in quantum mechanics, namely the infinite one-dimensional well, although such a point of view can be seriously questioned (for instance, what about the Heisenberg equations of motion for the infinite well?). Indeed, when going beyond academic elementary questions, this problem is *not* simple, and even turns out to be somewhat tricky, all subtleties obviously originating from the infinite discontinuities of the potential, which generates an infinity of bound states with an energy E_n increasing without limit like the square of the quantum number n. This immediately means that the propagator involves Gauss series (the Jacobi ϑ_3-function being one very special case [1]), which are known to possess quite uncommon features; as an example, Holschneider [2] shows that when the coefficients c_n of the series are $\propto n^{-2}$, the sum is a self-similar function in a precisely defined sense. Here, I only aim to give a brief account of intriguing results, together with a far-from-being-complete theoretical explanation and proof.

As all soluble simple models, the infinite well has been (and still is) the subject of numerous papers, aiming at pointing out specific features of quantum behaviour and also to closely analyse the classical limit (see, e.g., [3]) in a framework where detailed calculations can be performed in details without approximations. With this in mind, one basic question is the quantum-revival problem [4–6] (for a recent review, see [7]), which can be viewed as a quantum version of the Poincaré recurrence theorem and amounts to settle the role of the quasi-periodic functions appearing in the mathematical description of the problem at hand. This can be done under definite assumptions, namely that the expansion of the wavefunction on the eigensolutions has a resonant behaviour near an integer $n_0 \gg 1$ and a width $\Delta n \ll n_0$; then by making a Taylor expansion of each phase factor $e^{-iE_n t/\hbar}$ around n_0, it is possible to define the so-called classical period and a revival time [4]; the central point is that such an expansion generates a Gauss series for the (approximate) propagator, which is at the heart of the problem. The classical period thus defined is nothing else but the starting point of Heisenberg in constructing his Matrix mechanics. Clearly, these natural time scales are relevant only when such strong assumptions are done.

These points are not at all the subject of the present paper. The analysis done below does not rely on any large quantum numbers assumption; in addition, as shortly stated below, the dynamics of the problem here studied is so trivially periodic, for any initial state, that it deserves no discussion at all. On the other hand, it appears that some connections can be established with the *fractional* revival problem [8, 9], due to the fact that, at some definite times, the probability density turns out to be made up with transformed pieces of the initial (periodic) wave packet (see section 4, especially figure 7). The basic reason is that the propagator is here *exactly* given by a Gauss series.

The problem analysed below can also be viewed as the opposite one discussed by Bender *et al* [10], where a barrier is suddenly inserted within an infinite well. These authors show that the resulting dynamics strongly depends whether the barrier is located at a static node of the wavefunction or not, and explain how this situation mimics an EPR experiment based on energy conservation rather than angular-momentum conservation. They also demonstrate the fractal nature of the subsequent wavefunction, a property which basically results from the exact n^2 dependence of the energy spectrum and can be related to the work by Holschneider [2].

Fractal properties of the dynamics in an infinite well were recognized and analysed some time ago by Berry [11]; since that time, many papers have been devoted to the study of quantum carpets, fractional revivals and their formal relations with the classical Talbot effect [12–15], fractional or not.

To be sure and strictly speaking, infinite discontinuities can be discarded on physical grounds, but they conveniently modelize a situation where the depth V_0 of the well is much greater than all other relevant energies, and where the space variation of the potential occurs on a length scale l much smaller than all the others. Be it said in passing, for this reason, the classical limit of the infinite well is not a trivial point, due to the fact that one should first properly consider on the same level the two limits $l \to 0$ *and* $V_0 \to +\infty$, in order to check whether they commute or not and, if they do not, to choose the physically relevant limiting procedure for the considered case (for another example, see [16], section 1.6). On a technical level, the main qualitative change with regards to a finite well is the transformation of infinite series into finite discrete sums, completed with an integral over unbound states. This can be understood by locating the singularities of the Green's function in the complex plane and is readily accounted for by the use of the residue theorem (for an example, see [17]). When the number of bound states is large, the additional terms arising from the move of singularities are small; this fact technically explains the relevance of an idealized infinite well to describe real-life systems, as well in atomic as in condensed-matter physics.

Let me now precisely state the problem at hand, which corresponds to the following physically meaningful situation. Given that the particle (mass m) is initially in its ground state, the well is instantaneously (say, at $t = 0$) expanded to a larger size ($a \to \lambda a$, with $\lambda > 1$): what is the subsequent evolution of such a prepared initial state in the enlarged well? Some aspects of the dynamics in an infinite well with a moving boundary have already been studied [22–25]; here I focus on results which are absent from these works and, up to my knowledge, seem unquoted in the literature. Obviously, any possible connection with an experiment would first of all require a proper analysis of various time scales, in order to be sure that the following theoretical framework is relevant to the experimental device. A short discussion on this point is given in section 6.

Let us now enter into the specific problem and precise the notations used throughout. Taking, for the non-expanded well, $V(x) = 0$ if $0 < x < a$ and $V(x) = \infty$ elsewhere, the normalized eigenfunctions are

$$\psi_n(x) = \sqrt{\frac{2}{a}} \sin \frac{n\pi x}{a} \quad (0 \leqslant x \leqslant a), \tag{1.1}$$

and vanish outside this interval; the eigenenergies are

$$E_n = \frac{n^2\pi^2\hbar^2}{2ma^2} \equiv n^2\hbar\omega_1 \equiv n^2\frac{h}{T_1}, \tag{1.2}$$

where n is a strictly positive integer, whereas T_1 is trivially the smallest time period of any time-dependent state built as a linear combination of ψ_n's.

Since the initial state $\Psi(x, 0) \equiv \psi_1(x)$ is not a stationary state of the dilated well, $\Psi(x, t)$ has a non-trivial time dependence and, among other things, expectation values of the observables which do not commute with the Hamiltonian at $t > 0$ show up actual time dependence. I will focus on two of them, namely the probability density $\rho(x, t)$ and the density probability current $j(x, t)$ defined as usual:

$$\rho(x, t) = |\Psi(x, t)|^2, \qquad j(x, t) = \frac{\hbar}{m}\mathrm{Im}[\Psi^*(x, t)\partial_x\Psi(x, t)], \tag{1.3}$$

where Im denotes the imaginary part. ρ and j are related by the local conservation equation $\partial_t\rho + \partial_x j = 0$; considering only the density, as is most often done, provides an incomplete view of the dynamics, due to the interplay of these two basic quantities. A simple glance at the figures showing the variation of the current (see, e.g., figures 4 and 8) convinces that the latter deserves some attention. In addition, a few results concerning the averages of the position and the momentum of the particle will be briefly quoted at the end of the paper.

On the other hand, the expectation value of the energy does not change since no work is done on the particle when the well is expanded—which clearly shows why the present problem is the opposite of that discussed by Bender *et al* [10]; this obvious physical fact will be analytically checked in due time. As for the variance of the energy, it vanishes before the expansion, but turns out to be infinite once the latter has been performed (see section 5), simply because the energy probability distribution is a power law of the Pareto type with a rather small exponent.

2. Wavefunction at $t > 0$

The eigensolutions of the expanded well are simply obtained by making $a \to \lambda a$ in formulae (1.1) and (1.2), namely:

$$\psi_{\lambda,n}(x) = \frac{1}{\sqrt{\lambda}}\psi_n\left(\frac{x}{\lambda}\right), \qquad 0 \leqslant x \leqslant \lambda a; \qquad E_{\lambda,n} = \frac{1}{\lambda^2}E_n. \tag{2.1}$$

Note that if λ^2 is an irrational number, the two spectra E_n and $E_{\lambda,n}$ have no coincidence at all. The dilatation of the well lowers each eigenenergy and yields an increased energy density (in infinite space, the spectrum is continuous).

The resulting state at time $t > 0$, $\Psi(x, t)$, can be developed on the complete eigenstates $\{\psi_{\lambda,n}\}_n$ and has an expansion of the form

$$\Psi(x, t) = \sum_{n=1}^{+\infty} c_n\, \mathrm{e}^{\frac{1}{\mathrm{i}\hbar}E_{\lambda,n}t}\psi_{\lambda,n}(x). \tag{2.2}$$

Note that, as discussed at length by Styer [3] in connection with the classical limit, it immediately results that the motion is periodic, with the period $T = \lambda^2 T_1$, since the expansion of $\Psi(x, t)$ only contains integer multiples of the circular frequency $\omega_\lambda = \lambda^{-2}\omega_1$ (the square of an integer is an integer); as obvious on physical grounds, enlarging the well *increases* the period of the motion: for an infinite expansion, the motion is not periodic since, among other things, the wave packet would spread out *ad infinitum*. Also note that the wavefunction at time t is given by a Gauss series, i.e. a trigonometric series with time-oscillating factors of the form $\mathrm{e}^{\mathrm{i}n^2\omega t}$, as contrasted to $\mathrm{e}^{\mathrm{i}n\omega t}$ in a Fourier series. This yields quite rapid and irregular variations in time, all the more when the series coefficients decrease slowly with n, which is the case here (see equation (2.3)).

The coefficients c_n are readily found by writing the initial condition $\Psi(x, 0) = \psi_1(x)$ and are equal to the scalar products $\langle\psi_{\lambda,n}|\psi_1\rangle$; a straightforward integration yields

$$c_n = \frac{2\lambda^{3/2}}{\pi}\frac{\sin\frac{n\pi}{\lambda}}{\lambda^2 - n^2}, \tag{2.3}$$

so that the wavefunction at time $t \geqslant 0$ can be eventually written as

$$\Psi(x, t) = \frac{\mathrm{i}\lambda}{\pi}\sqrt{\frac{2}{a}}\sum_{n=-\infty}^{+\infty}\frac{\sin\frac{n\pi}{\lambda}}{n^2 - \lambda^2}\,\mathrm{e}^{\mathrm{i}\frac{n\pi x}{\lambda a}}\,\mathrm{e}^{-\mathrm{i}n^2\omega_\lambda t}, \tag{2.4}$$

an expression valid for $0 \leqslant x \leqslant \lambda a$, it being understood that $\Psi(x, t)$ vanishes outside the enlarged well. The expression (2.3) illustrates an obvious physical fact: for $\lambda \gg 1$, a huge number of excited states are relevant, although the inequality $\Delta n \ll n_0$ is not satisfied since then $\Delta n \sim \lambda \sim n_0$. For this reason, the problem here analysed cannot be so simply related to the classical limit studied elsewhere [4–6].

For any given time t, $\Psi(x, t)$ is a continuous function of x and of t; this is recognized from the fact that the coefficients c_n behave like n^{-2} for large n, ensuring that the series in (2.4) is uniformly convergent. Obviously, this is not true for the x- or t-derivatives of $\Psi(x, t)$ (remember that the potential has *infinite* discontinuities).

By construction, each exponential function $e_n(x, t) \equiv \mathrm{e}^{\mathrm{i}(\frac{n\pi x}{\lambda a} - n^2\omega_\lambda t)}$ satisfies the Schrödinger equation $\mathrm{i}\hbar\partial_t e_n = -\frac{\hbar^2}{2m}\partial_{xx}e_n$, so that $e_n^*\partial_{xx}e_n - e_n\partial_{xx}e_n^* = 0$: as it is the case for any stationary state in one dimension, the corresponding probability current is constant in space, $\partial_x j_{\mathrm{st}}(x) = 0$ (for bound states, one even has $j_{\mathrm{st}}(x) = 0$). This entails that performing a term-by-term derivation of the expansion (2.4) to get the formal expression of the current $j(x, t)$ related to $\Psi(x, t)$ can only generate singular terms, arising from the difference between the derivative of a function, and the series of the derivatives; these singularities turn out to be Dirac functions, which means that, for a given time, $j(x, t)$ is a piecewice constant function of x, whatever the initial state may be. Several examples of this will be given in due time.

Note that making $t = 0$ on the RHS of (2.4) leads to the function equal to $\sqrt{2/a}\,\sin(\pi x/a)$ for $0 \leqslant x \leqslant a$, and equal to zero for $a \leqslant x \leqslant \lambda a$, since $\Psi(x, 0) = \psi_1(x)$: in view of the following and considering the whole interval $[0, \lambda a]$, this allows us to say (trivially at this point) that the initial probability density shows up a *plateau* with a vanishing value for $a \leqslant x \leqslant \lambda a$. From this, one concludes that the following equality holds true for any $x \in [0, \lambda a]$:

$$\frac{\mathrm{i}\lambda}{\pi} \sum_{n=-\infty}^{+\infty} \frac{\sin \frac{n\pi}{\lambda}}{n^2 - \lambda^2}\, \mathrm{e}^{\mathrm{i}\frac{n\pi x}{\lambda a}} = \theta(a - x) \sin \frac{\pi x}{a}, \tag{2.5}$$

where $\theta(x)$ is the unit-step function ($\theta(x < 0) = 0$ and $\theta(x > 0) = 1$), as well as all the other equalities obtained by a term-by-term derivation; all of them can be $2\lambda a$-periodized in x if needed. The important point to realize is that the series on the LHS of (2.5) is identically zero for any x such that $a \leqslant x \leqslant \lambda a$ (it turns out unnecessary to define the step function for $x = 0$, since all the corresponding terms are multiplied by functions vanishing at this point). Note that if $\lambda \to 1$ (no change of the well), all coefficients go to zero, except for c_1 which equals 1, as it must be. More generally, if λ is a positive integer n_0, the indetermination for c_{n_0} is left by setting $\lambda = n_0 + \varepsilon$ and by taking the limit $\varepsilon \to 0$; one thus obtains $c_{n_0} = \frac{1}{\sqrt{n_0}}$.

As we will see, one remarkable thing is that the probability density at time t also shows up *plateaux* (but not always with a *vanishing* value), in other finite intervals $[x_k, x_{k+1}]$ at given periodic times; this can be figured out as the recurrent ghosts of the initial flatness on $[a, \lambda a]$. Berry [11] considered the case of a static well with a flat initial state and found that, in such an extreme case and at some definite times, the density is an indeed piecewise constant (discontinuous) function of x.

Also note from (2.4) that $\Psi(x, T - t) = \Psi^*(x, t)$, so that $\rho(x, t) = \rho(x, T - t)$: at times t and $T - t$ the two density distributions coincide, but since the two wavefunctions are complex conjugate, the two corresponding wave packets have *opposite* group velocities; for the same reason the current satisfies $j(x, T - t) = -j(x, t)$. Other symmetry properties can be found by inspection of the series (2.4); for example, one easily sees that for $t = T/4$, $\Psi(x, T/4) = -\Psi^*(\lambda a - x, T/4)$, namely that at a quarter of the period (or at three-quarter), the density profile is even with regards to the middle of the dilated well. Other relations exist when both the abscissa and the time are changed, for instance one has

$$\Psi(x, t + T/2) = -\Psi(\lambda a - x, t) \tag{2.6}$$

for any x and t. As we shall see, such symmetries play an important role, in particular to get closed convenient expressions for density and current at some remarkable times.

Since the initial state $\psi_1(x)$ is normalized to unity, so is $\Psi(x, t)$ at any time; this can be checked by a direct summation of the series $\sum_{n=1}^{+\infty} |c_n|^2$ (see appendix A).

3. Probability density plateaux and hints for a theoretical explanation

The surprise comes when plotting the probability density $\rho(x, t)$ at different times. Some examples are given in figures 1–3, which show that for very special times the probability density assumes *constant values* in some definite intervals included in $[0, \lambda a]$. As already said, these *plateaux* can be figured out as the echoes of the flatness of $\Psi(x, 0)$ with a zero height in the range $[a, \lambda a]$ for x.

The theoretical explanation of the existence of the *plateaux* lies on arguments which could be more firmly grounded if mathematical rigor were required. The basic idea is to

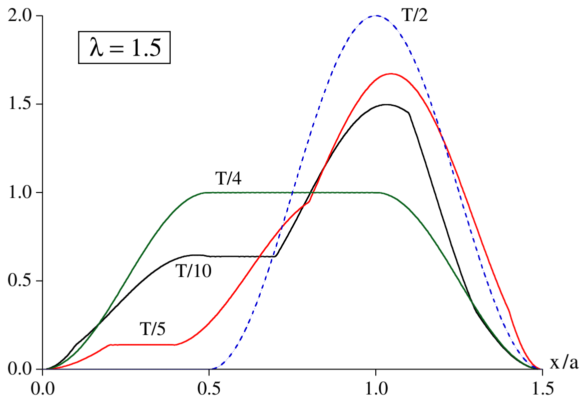

Figure 1. Probability density $|\Psi(x,t)|^2$ when the particle starts from the ground state of the undilated well; here, $\lambda = 1.5$. Each curve is labelled by the time t, with T being the period of the motion (see the text).

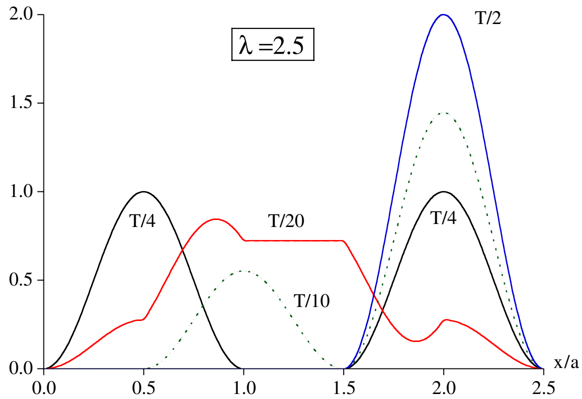

Figure 2. Same as figure 1 for $\lambda = 2.5$.

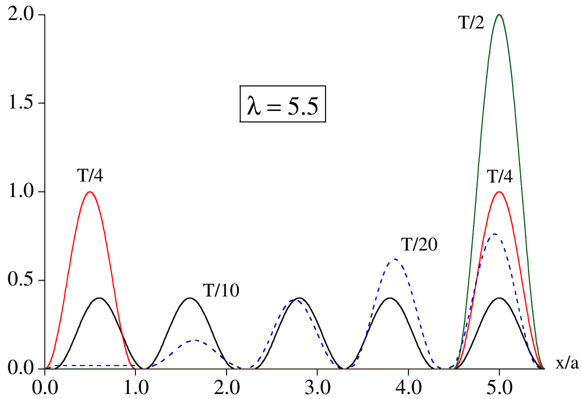

Figure 3. Same as figure 1 with $\lambda = 5.5$.

use the second derivative $\partial_{xx}\Psi(x,t)$ as an indicator, since its singularities determine the abscissae where $\Psi(x,t)$ can have a cusp. Indeed, let us assume for definiteness that x_0 is an abscissa to the left of which $\rho(x,t)$ is increasing and is constant on the right. This means that the first derivative $\partial_x\Psi$ has a negative jump at x_0, entailing that the second derivative contains an additive singular term $\propto\delta(x-x_0)$ with a negative weight, with $\delta(x)$ being the Dirac function (remember that if a function $f(x)$ has a jump Δf at $x=x_0$, its derivative is $f'(x)+\Delta f\,\delta(x-x_0)\equiv f'(x)+D_{\rm sing}f$, where f' is the ordinary derivative). At such a singular point, the derivative $\partial_x\Psi$ has a jump, so that, generally speaking, the density $|\Psi|^2$ shows up a cusp. Due to the general properties of the Schrödinger equation, singularities are indeed to be expected in the second derivative in the presence of infinite discontinuities of the potential; they merely reflect, on a quantum-mechanical level, the jumps of the velocity of a classical particle bouncing off the walls. These singularities, located at $x=0$ and $x=a$ at $t=0$, actually move about in the interval $[0,\lambda a]$ as time increases.

The second derivative of $\Psi(x,t)$ is obtained by a term-by-term derivation of the expansion (2.4); by writing $\frac{n^2}{n^2-\lambda^2}=1+\frac{\lambda^2}{n^2-\lambda^2}$, it can be recast in the form

$$\frac{\partial^2\Psi}{\partial x^2}=-\frac{\pi^2}{a^2}\Psi(x,t)+D^2_{\rm sing}\Psi, \tag{3.1}$$

where

$$D^2_{\rm sing}\Psi=-\frac{{\rm i}\pi}{\lambda a^2}\sqrt{\frac{2}{a}}\sum_{n=-\infty}^{+\infty}\sin\frac{n\pi}{\lambda}\,{\rm e}^{{\rm i}n\frac{\pi x}{\lambda a}}\,{\rm e}^{-{\rm i}n^2\omega_\lambda t} \tag{3.2}$$

is the only singular part of $\frac{\partial^2}{\partial x^2}\Psi$. The factor in the first term on the RHS of (3.1) is recognized as $-\frac{2m}{\hbar^2}E_1$ and comes from the (ordinary) Laplacian operator in the (time-dependent) Schrödinger equation. Now, keeping in mind the well-known Fourier expansion of the Dirac comb $\sum_{n\in\mathbb{Z}}{\rm e}^{2{\rm i}\pi nx}=\sum_{k\in\mathbb{Z}}\delta(x-k)$, it is realized that $D^2_{\rm sing}\Psi$ embodies Dirac functions whenever the series in (3.2) contains an infinite countable set of terms of the kind ${\rm e}^{{\rm i}\times{\rm integer}\times 2\pi}$, each having a coefficient which is independent of the dummy summation label. In order to explore this possibility, I rewrite the expression (3.2) as follows:

$$D^2_{\rm sing}\Psi=\frac{\pi}{\sqrt{2}\lambda a^{5/2}}\sum_{n=-\infty}^{+\infty}\left[{\rm e}^{{\rm i}\frac{n\pi}{\lambda a}(x-a)}-{\rm e}^{{\rm i}\frac{n\pi}{\lambda a}(x+a)}\right]{\rm e}^{-{\rm i}n^2\omega_\lambda t}. \tag{3.3}$$

First of all, note that for $x=a$, the first series in (3.3) reduces to $\sum_{n\in\mathbb{Z}}{\rm e}^{-{\rm i}n^2\omega_\lambda t}$, i.e. generates a Dirac comb whenever ${\rm e}^{-{\rm i}n^2\omega_\lambda t}=1$ for an infinite countable set of values for n; this is the case if $t=(p/q)T$ with p and q integers: for all values of n of the form kq (k integer), one has $n^2\omega_\lambda t=k^2qp\times 2\pi$, which of the desired form: integer $\times\,2\pi$. At this stage, and considering only the first series in (3.3), it is seen that a cusp *can* occur for $\Psi(x,t)$, with $(\partial_x\Psi)_{a+}-(\partial_x\Psi)_{a-}>0$ since the weight of $\delta(x-a)$ is then clearly a positive quantity. Note that the same argument also holds for all the points of the form $\frac{x-a}{\lambda a}=$ even integer but all the corresponding abscissae are outside the relevant interval $[0,\lambda a]$ and may be ignored.

This tells us that $x=a$ is a good candidate, but this is just the beginning of the story, due to the existence of the second series in (3.3). To show what can happen, let us set $x=a$ in both exponentials; the whole series then writes $\sum_{n\in\mathbb{Z}}(1-{\rm e}^{2{\rm i}n\pi/\lambda})\,{\rm e}^{-{\rm i}n^2\omega_\lambda t}$. In fact, it can happen that for all countably set of 'good' values of the integer n the two exponentials cancel each other, annihilating the possibility for the point $x=a$ to be a cusp. For definiteness, and as an example, let us go back to figure 1 and consider the curve $t=T/2$ where the density clearly shows up a 'normal' maximum at $x=a$. For this case, one has $p=1$ and $q=2$ in the above notations, which entails that the good values for n are $n=2s$ (s integer); then, the only non-vanishing factors $(1 - e^{2in\pi/\lambda})$ are for $s = 1, 2(3)$, but for $s = 1(3)$ and $s = 2(3)$ they have opposite signs, so that the two related Dirac combs indeed have opposite weights, and the singularity at $x = a$ disappears. Thus, the point $x = a$ is not *always* such a remarkable point.

Let us now show that other values of the couple (x, t) can define the edges of the *plateaux*, without trying to give an exhaustive catalogue of all these possibilities, just aiming at giving a few sufficient conditions for that.

The second exponential term $e^{in\pi(x+a)/(\lambda a)}$ in (3.3) is equal to 1 for any n if $(x+a)/(\lambda a) = r/s$, r and s integers, and if n is an even multiple of s; the constraint $0 \leqslant x \leqslant \lambda a$ entails $1 \leqslant r/s \leqslant 1 + 1/\lambda$. This being realized, the conditions for the time-varying factor $e^{-in^2\omega_\lambda t}$ are the same as above, namely t must be a rational fraction of the period T: $t = (p/q)T$.

One example of such a case can be seen in figure 1, where $\lambda = 3/2$. For $t = T/4$ $(\omega_\lambda t = 2\pi/4)$, $p = 1, q = 4$ in the above notations. Close inspection reveals that $x = a$ is indeed a cusp, as well as $x = a/2$ (take $r = s = 1$); there is numerical evidence, and this is analytically proved below, that these points are in fact the edges of a *plateau*. Note that the signs of the Dirac combs can be reversed; for instance with $(x+a)/(\lambda a) = r/s$, if r is odd and n an *odd* multiple of s, $e^{i(2k+1)s\pi(r/s)} = e^{i(2k+1)r\pi} = -1$ (as examples, see the curves $t = T/5$ and $T/10$ in figure 1, for which the density increases on the left and to the right of the *plateau*).

Obviously, the existence of cusps is just a necessary condition for the occurrence of the *plateaux*. In order to analytically demonstrate their existence, one must generally prove that between two so identified given cusps the density is indeed constant. This seems to be a rather intricate and difficult mathematical problem; in this short preliminary paper, I just intend to demonstrate this in a few specific cases, hoping to give a complete general proof in a future article.

Before going further, a comment turns out to be useful. The basic ingredients of the present analysis are first the Dirac comb, second the apparition of the constant-density *plateaux*. With all this together, it is tempting to establish a relation with recent findings in the research of attosecond spectroscopy (for an introduction, see [18]), especially with the constant intensity distribution for a large number of harmonics, usually called *frequency comb* because of its similarities with a true Dirac comb. Such an analogy should not be pushed too far. A first observation is that the generation of harmonics in a nonlinear medium can be explained in a semi-classical theory [19], even if a purely quantum-mechanical theory is available [20]; in contrast, as is hopefully clear, the density *plateaux* here result from a subtle interplay between essentially complex amplitudes, the phases of which play a crucial role for the onset of the former. Another difference is that the words *characteristic plateau* in attosecond spectroscopy merely express the fact that the intensity I_n of the nth harmonic is nearly constant for n going from a small integer number to a few hundreds; this is frankly different from the strictly constant values in definite intervals for x found above for the continuous density of probability $\rho(x, t)$. Also note that, as explained above, the Dirac comb is just a technical tool for hunting singularities (divergences), which anyway are connected to the second derivative of the wavefunction, not to the squared modulus of the latter.

As for the frequency comb on the femtosecond scale now used for metrology of optical frequencies [21], no connection of any kind can be established since it this case there are no *plateaux* at all.

4. Closed expressions for specific times

It turns out that for some definite times t_k closed expressions of the wavefunction $\Psi(x, t_k)$ can be written. I will here consider only the three cases $t = T/2^{N+1}$ with $N = 0, 1, 2$, before showing the existence of a phenomenon, namely the fragmentation of the wave packet and the existence of regular patterns when λ is above a characteristic threshold λ_c, depending on the specific time considered. The basic idea is to play with the time phase factors appearing in the expansion (2.4) and to express $\Psi(x, t_k)$ as a linear combination of the known initial wavefunction taken at different abscissae x_i. The generalization for times of the form $(p/q)T$ (p and q integers, $p < q$, p and q prime numbers) seems quite feasible, although it promises to be somewhat cumbersome as long as a more elegant method is not available.

A first observation is the following: at half of a period ($t = T/2$), a simple glance at the series (2.4) shows that $\Psi(x, T/2) = -\Psi(\lambda a - x, 0)$, which is just the symmetry relation (2.6) for $t = 0$; now, since $\Psi(x, 0) \equiv \psi_1(x)$, this equality gives a closed simple expression for the wavefunction at this remarkable time. In the following, I show how such a method can be used for the other times defined above.

4.1. *The case $t = T/4$*

The case $\lambda = 3/2$ (see figure 1) and the spectacular *plateau* occurring for $t = T/4$ draws attention on this peculiar time. To start with and to introduce the method, let us analyse the things in details, but for any λ. The clue is simply to realize that at this time the time-dependent exponential in (2.4) is equal to 1 if n is even and to $-\mathrm{i}$ if n is odd. This allows us to write $\Psi(x, T/4)$ in the form

$$\Psi(x, T/4) = S_{2,0}(x) - \mathrm{i}S_{2,1}(x), \tag{4.1}$$

where the two (real) sums $S_{2,0}$ and $S_{2,1}$, respectively ,correspond to even and odd values for the summation index n. Now that all the time factors on the RHS of (4.1) are fixed, it is tempting to compare this expression with $\Psi(x, 0)$; noting that $\Psi(x, 0) = S_{2,0}(x) + S_{2,1}(x)$ and $\Psi(\lambda a - x, 0) = -S_{2,0}(x) + S_{2,1}(x)$, the two sums $S_{2,k}$ can be expressed in terms of $\Psi(x, 0)$, thus readily obtaining the sum of the series (2.4) at this time (setting $\xi = x/a$ for simplicity):

$$\Psi(x, T/4) = \frac{1}{\sqrt{a}}[\mathrm{e}^{-\mathrm{i}\pi/4}\theta(1-\xi)\sin\pi\xi - \mathrm{e}^{+\mathrm{i}\pi/4}\theta(1-\lambda+\xi)\sin\pi(\lambda-\xi)], \tag{4.2}$$

an equality which yields the closed simple expression of the density for any λ:

$$a\rho(x, T/4) = \theta(1-\xi)\sin^2\pi\xi + \theta(1-\lambda+\xi)\sin^2\pi(\lambda-\xi), \tag{4.3}$$

with still $0 \leqslant x \leqslant \lambda a$. Taking $\lambda = 3/2$, (4.3) immediately gives

$$a\rho(x, T/4) = \begin{cases} \sin^2\pi\xi, & 0 \leqslant x \leqslant a/2 \\ 1, & a/2 \leqslant x \leqslant a \\ \cos^2\pi\xi, & a \leqslant x \leqslant 3a/2 \end{cases} \tag{4.4}$$

which proves the existence of the *plateau* between $a/2$ and a in this definite case. Note that this density is built in the following way: take the initial density, cut it into two pieces in the middle, translate the right part to the right of the distance a, draw a horizontal line between the two *maxima* and divide the whole by a factor 2. We will recover such rules below, showing that the density at some other remarkable times can be built by playing with the pieces of the initial density.

The expression (4.3) holds true at $t = T/4$ for any λ and has two clear-cut behaviours according to $\lambda < 2$ or $\lambda > 2$. In the first case, the two θ functions are simultaneously non-zero in the interval $[(\lambda-1)a, a]$, so that

$$a\rho(x, T/4) = \begin{cases} \sin^2\pi\xi, & 0 \leqslant x \leqslant (\lambda-1)a \\ \sin^2\pi\xi + \sin^2\pi(\lambda-\xi), & (\lambda-1)a \leqslant x \leqslant a \\ \sin^2\pi(\lambda-\xi), & a \leqslant x \leqslant \lambda a. \end{cases} \tag{4.5}$$

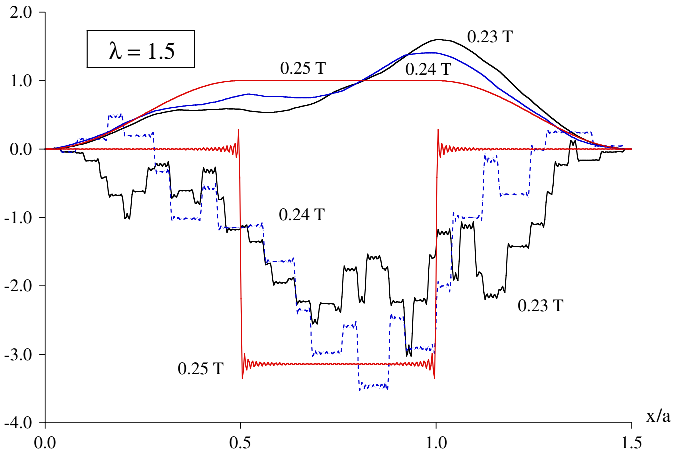

Figure 4. Probability density (upper smooth curves) and density current (lower piecewise constant curves) for three very close times near $t = T/4$. Note the extreme variability of the current in space (except at exactly a quarter of a period). The oscillations near the jumps arise from numerical truncations of the series and are obviously related to some kind of Gibbs phenomenon adapted to a Gauss series.

This shows that for $1 < \lambda < 2$ but $\lambda \neq 3/2$ the function at $T/4$ has no *plateau*; in fact, for all such values of λ, numerical plots show that the latter does exist, but for other times and not located between the two simple values $a/2$ and a. Clearly, the relative simplicity of the $\lambda = 3/2$ case is due to the fact that λ is a 'simple' rational number.

Note that the x-derivative of the density is equal to the real part $\mathrm{Re}(\Psi^* \partial_x \Psi)$; one easily checks from the expression (4.2) that, for $\lambda < 2$ (and still $t = T/4$), $\mathrm{Re}(\Psi^* \partial_x \Psi)$ never identically vanishes in a finite interval. Also note that if $\Psi(x, T/4)$ as given by (4.2) is a continuous function of x (as it must be), its x-derivative is not, although it is devoid of Dirac peaks due to the cancellation of $\Psi(x, t)$ at each jump of the derivative.

For $\lambda > 2$, the two intervals $[0, a]$ and $[(\lambda-1)a, \lambda a]$ do not overlap; then, expression (4.3) says that the wavefunction identically vanishes at $t = T/4$ for any $x \in [a, (\lambda-1)a]$. Examples of this are illustrated in figures 2 and 3; it is seen that $|\Psi|^2$ vanishes between a and $3a/2$ for $\lambda = 2.5$, and between a and $9a/2$ if $\lambda = 5.5$. Thus, for $t = T/4$ and $\lambda > 2$, the wave packet splits itself in two distant parts: the particle is fully localized in two intervals separated by a finite one; in each of them, the profile is the clone of the initial one, just divided by 2. This *fragmentation* into identical curves will also occur for $t = T/8$: then, four identical well-separated clusters are found, provided that λ is greater than 4 (see section 4.3), each of them being just one quarter of the initial density $|\psi_1(x)|^2$ properly translated.

As explained above, the current probability density $j(x, t)$ is a constant piecewise function, generally having jumps when the first derivative of the wavefunction is discontinuous; otherwise stated, the jumps of $j(x, t)$ also occur whenever the singular part $D^2_{\mathrm{sing}}\Psi$ contains a Dirac comb. This turns out to happen in many points of the interval $[0, \lambda a]$, as seen in figure 4, where all the functions have been numerically computed from the series (2.4). These plots also show that there is not necessary a direct relation between the jumps of the current and the edges of the *plateaux* and reveal the irregular variation of $\partial_x \Psi$, which is not always clearly visible on the plot of the density, all the more since a cusp can occur only if $\mathrm{Re}(\Psi^* \partial_x \Psi) \neq 0$.

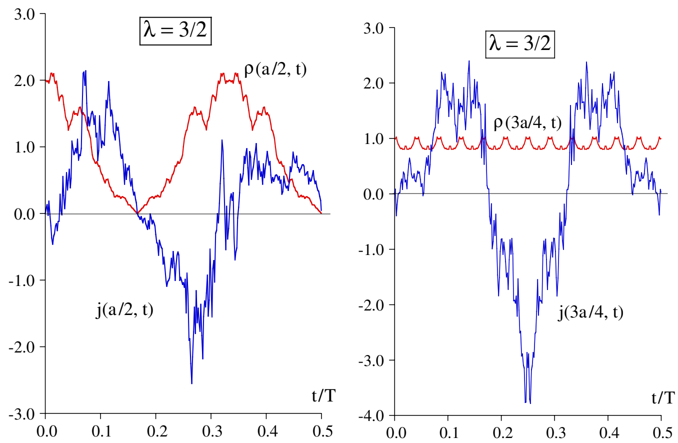

Figure 5. Probability density ρ and current j as a function of time at $x = a/2$ (left), middle of the well before the expansion, and $x = 3a/4$ (right), middle of the well after the expansion.

Now, starting from (1.3) with $\Psi(x, T/4)$ given by (4.2), a straightforward calculation yields the piecewice constant expression

$$j(x, T/4) = \frac{\pi\hbar}{ma^2}\theta(1-\xi)\theta(\xi-\lambda+1)\sin\pi\lambda. \tag{4.6}$$

Again, the situation is quite different for $1 < \lambda < 2$ and for $\lambda > 2$. In the first case, the current vanishes for $0 < x < (\lambda-1)a$ and for $a < x < \lambda a$; in the middle interval, it assumes the constant negative value $\frac{\pi\hbar}{ma^2}\sin\pi\lambda$. Due to the conservation equation, the two points $x = (\lambda-1)a$ and $x = a$ are the only points where, at $t = T/4$, the time partial derivative $\partial_t\rho$ is non-zero. As contrasted, for $\lambda > 2$, the current vanishes everywhere: not only at this time the wave packet is split off in two fully disconnected parts, but the current between both regions is identically zero since there the wavefunction strictly vanishes.

I mentioned above that, due to the central role of the Gauss series given in (2.4), it is expected that all quantities have a rather rapid and irregular variation in time. Such a fact is illustrated in figures 5 and 6, where the probability density and current are plotted for a fixed x as functions of time (remember that for t and $T-t$ the densities are the same and the currents have reversed signs). At first glance, $j(x,t)$ even looks like a singular function; remember that j is given by a double Gauss series. For $\lambda = 3/2$, one has the symmetry $j\left(\frac{a}{2}, t\right) = j\left(a, \frac{T}{2}-t\right)$.

4.2. The case $t = T/8$

I shall here follow the same arguments as before, the situation being a bit more complex. I first introduce four sums $S_{4,k}$ $(k = 0, 1, 2, 3)$ corresponding to the values $n = 4p - k$ of the dummy summation variable in the series (2.4). Now, inspection of the time phase factors shows that one has

$$\Psi(x, T/2^{N+1}) = \sum_{k=0}^{2^N-1} \mathrm{e}^{-\mathrm{i}k^2\pi/2^N} S_{2^N,k}(x), \tag{4.7}$$

which has now the form of a Gauss *sum* (not a series). For $N = 2$, this gives

$$\Psi(x, T/8) = S_{4,0}(x) - S_{4,2}(x) + \mathrm{e}^{-\mathrm{i}\pi/4}[S_{4,1}(x) + S_{4,3}(x)]. \tag{4.8}$$

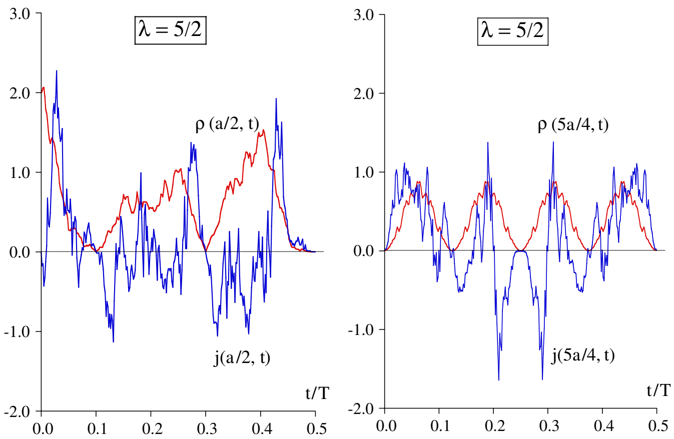

Figure 6. Same as figure 5 for $\lambda = 5/2$. $x = a/2$ (left), middle of the well before the expansion, and $x = 5a/4$ (right), middle of the well after the expansion.

I now follow the same idea as before, trying to choose definite abscissae x_i such that the space factor in (2.4) compensates in some way the dephasing due to the time factor. By trial and error, it is seen that the proper abscissae x_i which allow us to express the various sums in terms of the initial wavefunction $\Psi(x_i, 0)$ are $\lambda a/2 \pm x$ and $3\lambda a/2 - x$. First note that the sum $S_{4,1}(x) + S_{4,3}(x)$ is simply equal to the known quantity $S_{2,1}(x)$ already introduced in subsection 4.1; as for the difference $S_{4,0}(x) - S_{4,2}(x)$, I find the following:

$$0 \leqslant x \leqslant \frac{\lambda a}{2} : S_{4,0}(x) - S_{4,2}(x) = \frac{1}{2}\left[\Psi\left(\frac{\lambda a}{2} + x, 0\right) - \Psi\left(\frac{\lambda a}{2} - x, 0\right)\right], \tag{4.9}$$

$$\frac{\lambda a}{2} \leqslant x \leqslant \lambda a : S_{4,0}(x) - S_{4,2}(x) = \frac{1}{2}\left[\Psi\left(-\frac{\lambda a}{2} + x, 0\right) - \Psi\left(\frac{3\lambda a}{2} - x, 0\right)\right]. \tag{4.10}$$

Great care must be exercised when writing the relations between the sums $S_{2^N,k}$ and the values $\Psi(x_i, 0)$ due to the fact that the equality (2.5) *only* holds for $0 \leqslant x \leqslant \lambda a$: outside this interval, the wavefunction vanishes, although this is not the case for the sums since they are $2\lambda a$-periodic functions.

The above results eventually allow us to write the following closed expression for $\Psi(x, T/8)$ valid for any λ:

$$\sqrt{2a}\Psi(x, T/8) = \theta\left(\frac{\lambda}{2} - \xi\right) f_<(\xi) + \theta\left(\xi - \frac{\lambda}{2}\right) f_>(\xi) \\ + \mathrm{e}^{-\mathrm{i}\pi/4}[\theta(1-\xi)\sin\pi\xi - \theta(1-\lambda+\xi)\sin\pi(\xi-\lambda)], \tag{4.11}$$

where the two functions $f_<$ and $f_>$ are

$$f_<(\xi) = \theta\left(1 - \frac{\lambda}{2} - \xi\right)\sin\pi\left(\xi + \frac{\lambda}{2}\right) + \theta\left(1 - \frac{\lambda}{2} + \xi\right)\sin\pi\left(\xi - \frac{\lambda}{2}\right), \tag{4.12}$$

$$f_>(\xi) = \theta\left(1 + \frac{\lambda}{2} - \xi\right)\sin\pi\left(\xi - \frac{\lambda}{2}\right) + \theta\left(1 - \frac{3\lambda}{2} + \xi\right)\sin\pi\left(\xi - \frac{3\lambda}{2}\right). \tag{4.13}$$

Note that small times give more cusps than larger times; numerical runs confirm that the initial two cusps propagate through the interval $[0, \lambda a]$ and multiply at the very beginning of the motion, before reducing in number when the time gets closer to half of a period.

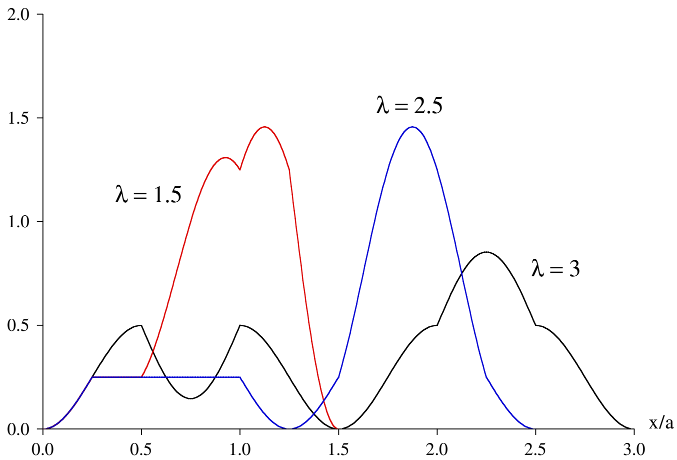

Figure 7. Probability density $\rho(x, T/8)$ calculated from the closed analytical expression (4.11), for three values of λ. Note the coincidence of the three densities for $0 \leqslant x \leqslant a/4$, and between $a/4$ and $a/2$ when $\lambda = 1.5$ and 2.5. The fact that the density is constructed with pieces of $|\Psi(x, 0)|^2$ is clearly visible for the case $\lambda = 3$.

In order to illustrate these results valid for any λ, let me take again $\lambda = 3/2$; then, the above formula gives for $2\sqrt{a}\Psi(x, T/8)$

$$0 \leqslant x \leqslant \frac{a}{4} : -(1 + \mathrm{i}) \sin \pi\xi, \tag{4.14}$$

$$\frac{a}{4} \leqslant x \leqslant \frac{a}{2} : -\mathrm{i} \sin \pi\xi - \cos \pi\xi, \tag{4.15}$$

$$\frac{a}{2} \leqslant x \leqslant a : -\mathrm{i} \sin \pi\xi - (2 - \mathrm{i}) \cos \pi\xi, \tag{4.16}$$

$$a \leqslant x \leqslant \frac{5a}{4} : -\sin \pi\xi - (2 - \mathrm{i}) \cos \pi\xi, \tag{4.17}$$

$$\frac{5a}{4} \leqslant x \leqslant \frac{3a}{2} : -(3 - \mathrm{i}) \cos \pi\xi. \tag{4.18}$$

This respectively gives the expressions for the dimensionless density $a\rho(x, T/8)$ in the corresponding five intervals: $\frac{1}{2}\sin^2 \pi\xi$, $\frac{1}{4}$, $\frac{1}{4} + \cos^2 \pi\xi - \frac{1}{4}\sin 2\pi\xi$, $\frac{1}{4} + \cos^2 \pi\xi + \frac{1}{2}\sin 2\pi\xi$ and $\frac{5}{2}\cos^2 \pi\xi$; note the *plateau* for $a/4 \leqslant x \leqslant a/2$, and the cusp at $x = a$, all features are apparent in figure 7 where the density $a\rho(x, T/8)$ using the preceding formula is plotted, and the analytical expression (4.11) for the other λ values. I checked that they give the same density as that obtained by a numerical calculation using directly the expansion (2.4).

Coming back to the general λ case, the expressions (4.11)–(4.13) show that $\Psi(x, T/8)$ *a priori* shows up cusps at the following abscissæ, which I precisely define for further reference:

$$x_1 = a, \qquad x_2 = |\lambda/2 - 1|a, \qquad x_3 = \lambda a/2,$$
$$x_4 = \theta(2 - \lambda)(3\lambda/2 - 1)a + \theta(\lambda - 2)(1 + \lambda/2)a, \qquad x_5 = (\lambda - 1)a. \tag{4.19}$$

Quite remarkably, they are equally spaced, being located at $pa/4$ ($p = 1, 2, 3, 4, 5$) for $\lambda = 3/2$; for $\lambda > 2$, where $(\lambda - 1)a$ and $\lambda a/2$ merge, the cusp at $(3\lambda/2 - 1)a$ gets out of the interval $[0, \lambda a]$, but the cusp at $(1 + \lambda/2)a$ comes in so that there is still five cusps, which all

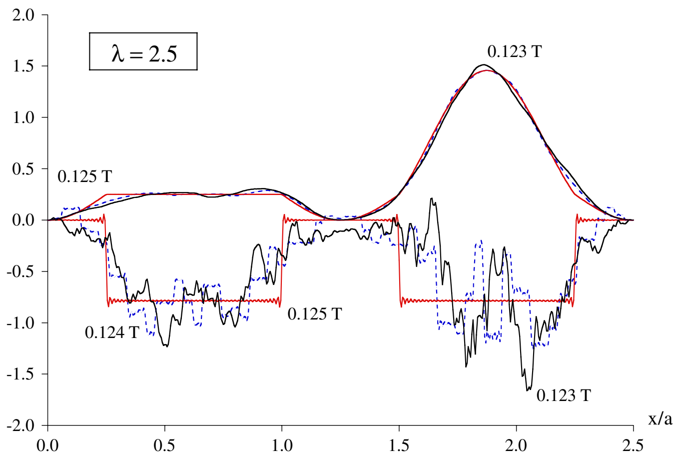

Figure 8. Probability density (upper smooth curves) and density current (lower piecewise constant curves) for three very close times near $t = T/8$.

remain in the latter interval for any λ (see figure 9). I will come back to this in the following subsection.

The current can also be easily computed; I find

$$j(x, T/8) = \frac{\pi\hbar}{2\sqrt{2}ma^2}\left[c_{1\pm}(\xi)\sin\frac{\pi\lambda}{2} + c_{3\pm}(\xi)\sin\frac{3\pi\lambda}{2}\right], \tag{4.20}$$

where the functions $c_{r\pm}$ depend on the considered interval; for $x < \lambda a/2$

$$c_{1-}(\xi) = \theta(1-\xi)\left[-\theta\left(1-\frac{\lambda}{2}-\xi\right) + \theta\left(1-\frac{\lambda}{2}+\xi\right)\right] + \theta\left(1-\frac{\lambda}{2}+\xi\right)\theta(1-\lambda+\xi) \tag{4.21}$$

and

$$c_{3-}(\xi) = \theta(1-\lambda+\xi)\theta\left(1-\frac{\lambda}{2}-\xi\right). \tag{4.22}$$

For $x > \lambda a/2$, one has

$$c_{1+}(\xi) = \theta\left(1+\frac{\lambda}{2}-\xi\right)[\theta(1-\xi)+\theta(1-\lambda+\xi)] - \theta\left(1-\frac{3\lambda}{2}+\xi\right)\theta(1-\lambda+\xi) \tag{4.23}$$

and

$$c_{3+}(\xi) = \theta(1-\xi)\theta\left(1-\frac{3\lambda}{2}+\xi\right). \tag{4.24}$$

All this shows that $j(x, T/8)$ is a piecewise constant function, as it must be. The density and the current are plotted in figure 8 from the (truncated) series (2.4) for three close times near $T/8$; note again the rapid variation of the current. For $\lambda > 4$, the current vanishes everywhere.

4.3. Fragmentation

One sees in figures 2 and 3, which both correspond to $\lambda > 2$, that for $t = T/4$ the wave packet is split into two symmetric parts at the edges of the allowed interval for x. This is true for any $\lambda > 2$, as a consequence of (4.3): then the two intervals $[0, a]$ and $[(\lambda-1)a, \lambda a]$ do not

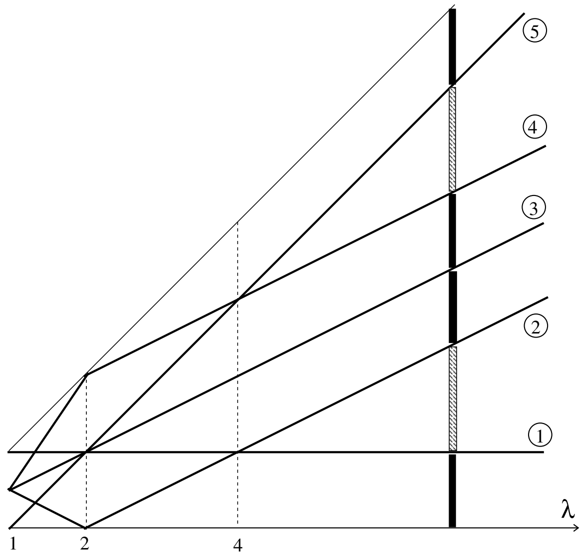

Figure 9. Abscissæ of the cusps as a function of λ. The black segments show the domains where the density is non-zero; and the hatched ones those where the density vanishes. Note that when λ is above the threshold $\lambda_c = 4$, the domains of non-vanishing density move away one from the other, but keep the same size and shape.

overlap, so that the density is non-zero only for $0 < x < a$ and $(\lambda - 1)a < x < a$; the two corresponding peaks are identical in shape, each equal to the initial density simply divided by 2. It thus turns out that for times $T/4$ (and $3T/4$) the particle is fully localized into narrow domains and cannot be found between them. It can be said that, provided the expanded well has a size large enough, namely greater than $2a$, there is the possibility for two identical bumps of width a localized at the edges of the box, with no density at all in between.

The same phenomenon occurs for $t = T/8$ (and $7T/8$): for $\lambda > 4$, the density shows up four identical peaks, each of width a. Two of them are at the edges of the interval $[0, \lambda a]$, and the two others are on each side of the middle of the box. Interestingly enough, the onset of the four peaks occurs at $\lambda = 4$, a threshold at which the cusps are equally spaced (two couples of them are degenerate because here $\lambda - 1 = 1 + \lambda/2$ and $\lambda/2 - 1 = 1$). Once this has happened, the two middle peaks ('twin peaks') remain at the fixed distance a one from the other when λ increases, being localized between $\lambda a/2 \pm a$ (central cusps), while the two edge peaks also remain unchanged and are still located between 0 and a, and $(\lambda - 1)a$ and λa as λ varies (see figure 10). It thus turns out that for λ above the critical value $\lambda_c = 4$, the cusps delineate the regions of vanishing and non-vanishing density: $\lambda a/2$ and $(\lambda/2 \pm 1)a$ for the central clusters, a and $(\lambda - 1)a$ for those localized near the boundaries of the box. Again, one can say that when the size is large enough (now greater than $4a$), four identical peaks of width a can take place as indicated and are independent of the expansion parameter λ.

To sum up this discussion, it can be stated that as far as λ is greater than 4, the density $\rho(x, T/8)$ is simply obtained by translating several times the initial density $|\psi_1(x)|^2 \equiv \rho(x, 0)$ according to the formula

$$\rho(x, T/8) = \frac{1}{4}\sum_{\alpha=1}^{4} \rho(x - l_\alpha, 0) \qquad (\lambda > 4), \tag{4.25}$$

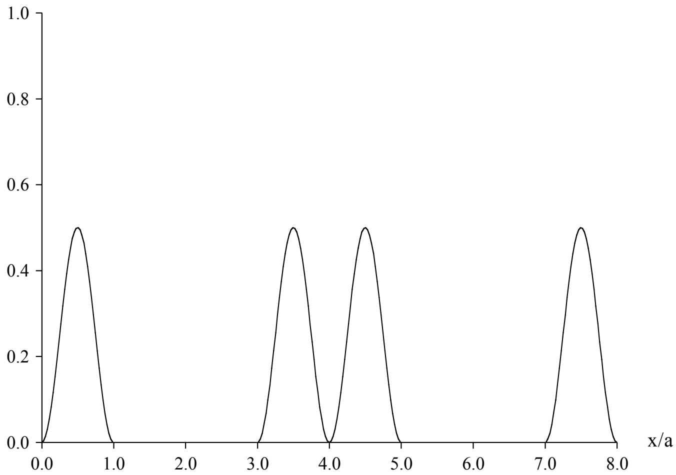

Figure 10. Probability density ρ at $t = T/8$, for $\lambda = 8$ above the critical value $\lambda_c = 4$. The fragmentation has occurred; the peaks now remain unchanged in size and shape when λ varies and are located at the edges of the box, and on either side of the middle.

where the locations of the maxima l_α are $a/2$, $(\lambda \pm 1)a/2$ and $(\lambda - 1/2)a$. Increasing the expansion factor does not alters the profile of each peak; the twin peaks stay locked around the centre of the box, whereas the edge peaks are getting more and more far away. Remember that above this threshold, the current identically vanishes everywhere.

Gathering the above results with those obtained in the $T/4$ case, one can anticipate that for all times of the form $T/2^{N+1}$ there exists a threshold $\lambda_c = 2^N$ above which a fragmentation into 2^N peaks occurs. The density profile consists of the elementary pattern $\frac{1}{2^N}\left[|\Psi(x,0)|^2 + \left|\Psi\left(\frac{\lambda a}{2^{N-1}} - x, 0\right)\right|^2\right]$, and its $2^{N-1} - 1$ clones translated by integer $\times\, \lambda a/2^{N-1}$; this is yet to be analytically proved in general, but numerical calculations allow us to be convinced that this is true for any N (see figure 11 for an example). All this also confirms that many cusps exist at first times of the T-periodic motion, but remember that the time unit is precisely the period $T = \lambda^2 T_1$, so that $t_N \equiv T/2^{N+1} = \lambda^2 T_1/2^{N+1} \geqslant 2^{N-1} T_1$: large N does not mean small times.

The above conjectures are performed in the continuity of the analytical results given in this paper. Many other statements can be claimed in view of numerical evidence, but they still remain to be proved; let me give a few of them follows:

(i) For all times of the form $t_M = T/M$, with M being an integer, there exists a threshold $\lambda_c(M)$ above which complete fragmentation occurs.
  If M is even, $\lambda_c(M) = M/2$ and one gets a pattern of $M/2$ peaks located as above. If M is odd, fragmentation starts up at $\lambda_c = M$, with M peaks; all peaks appear in twins except one, located near the origin.

(ii) Fragmentation also takes place at times pT/M, with p being an integer. The number of peaks depends on whether p and M have common divisors or not. For instance, with $M = 12$, $\lambda \geqslant \lambda_c = 6$, one finds six peaks if $p = 1, 5$, three peaks if $p = 2, 4$, two peaks if $p = 3$ and a single peak at $x = \lambda a$ if $p = 6$ (half-period).

The method presented in this paper should be still efficient for proving these (and other) statements, although a more elegant procedure is highly wishable in order to make the analysis less cumbersome and more systematic. Work in this direction is in progress.

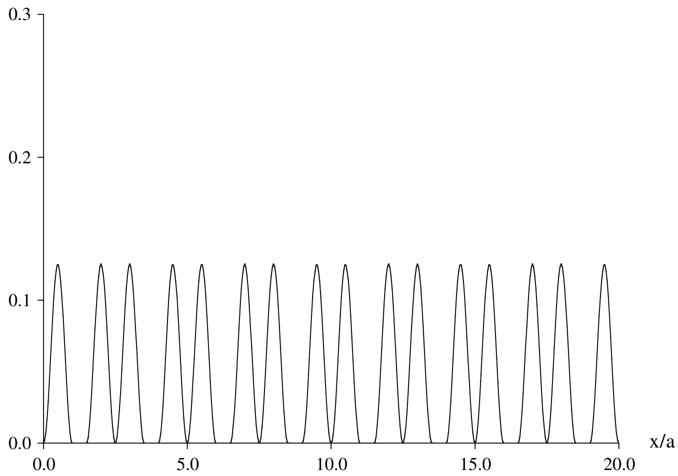

Figure 11. Probability density ρ at $t = T/2^{N+1}$ for $N = 4$ and $\lambda = 20$; here, the critical value is $\lambda_c = 2^4 = 16$.

Some of the above results can be summed up by saying that at definite times the density is made up with pieces of the initial density, some translated, some being reversed up to an additive constant. This construction game is reminiscent of the fractional revivals (exact or approximate) which can occur in a lot of quantum systems. Indeed, the fragmentation just found is one example of exact fractional revival, as precisely defined by Aronstein and Stroud in [8]: at some particular times, the density is a superposition of (renormalized) translated copies of the initial density (see equation (4.25) for an example). On the other hand, when the expansion parameter is not large enough (see, e.g., figure 7), the reconstruction of the density proceeds along much more complicated rules: the initial density has to be cut into definite pieces, which are moved away, some of them being turned upside down. Clearly, this leads to a graph which bears a faint resemblance only with the initial density and cannot be said to be a *revival* of the latter.

5. Other results

After having focused on these rather outstanding features of the wave packet dynamics, let me take the opportunity to add a few things for completeness, some of them being, as far as I know, unquoted in the literature.

As a first by-product, one can compute the probability $P_n(t)$ to find the energy $E_{\lambda,n}$ when achieving a measurement of the energy at a time $t > 0$; according to one of the postulates of quantum mechanics, one has $P_n(t) = |\langle\psi_{\lambda,n}|\Psi(t)\rangle|^2 = \frac{4\lambda^3}{\pi^2}\frac{\sin^2(n\pi/\lambda)}{(\lambda^2-n^2)^2}$; if λ is equal to an integer n_0, the probability P_{n_0} is equal to $1/n_0$. When $\lambda \gtrsim 1$, the distribution of P_n is an ever decreasing function of n; in contrast, if $\lambda \gg 1$, P_n has a maximum for $n \simeq \lambda$, but the probability distribution is quite flat (see figure 12). This maximum has a clear physical meaning: there is some kind of resonance in the vicinity of the states having an energy $E_{\lambda,n}$ close to E_1, the initial (and constant) value for the average energy. It can be checked that the expectation value $\sum_{n\in\mathbb{N}^*} P_n E_{\lambda,n}$ is indeed equal to E_1 at any time (see appendix A).

Note that the variance of the energy is infinite, since the average $\langle H^2\rangle$ is given by a diverging series ($P_n \propto n^{-4}$, $E^2_{\lambda,n} \propto n^4$). This is due to the fact that the prepared state

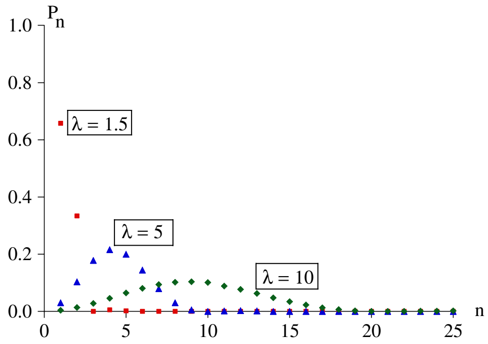

Figure 12. Probability distribution P_n for three values of λ.

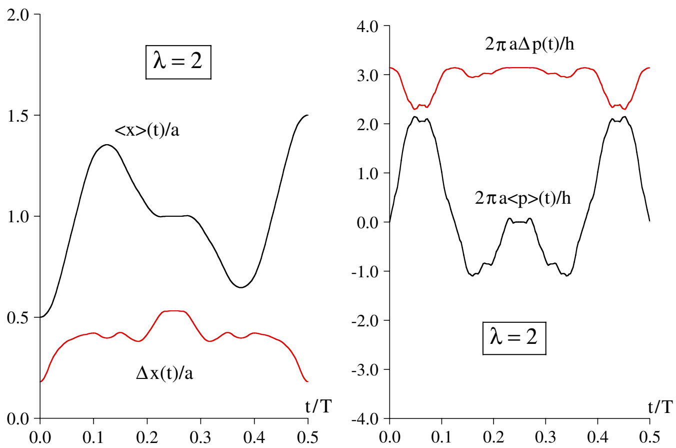

Figure 13. Left: variations in time ($0 \leqslant t \leqslant T/2$) of the expectation value of the coordinate and its variance. Right: same for the momentum.

effectively implies a large number of eigenstates $\psi_{\lambda,n}$ because the coefficients c_n have a slowly-decreasing algebraic n-dependence, so that high energies are relevant for any λ. This yields divergent energy fluctuations, exactly as in the case of a Pareto law with a small exponent.

The expectation values of the position, $\langle x\rangle(t)$, and of the momentum, $\langle p\rangle(t)$, also display interesting behaviour with time. An example is given in figure 13; it is seen that the particle is periodically at rest on the average, since $\langle x\rangle(t)$ is constant and equal to $\lambda a/2$ whereas $\langle p\rangle(t)$ vanishes. This means that repeated measurements at those specific times would give exactly the same results as if the particle was in *any* stationary state of the dilated well. Measuring (independently) the energy would actually reveal the true nature of the state, giving for each measure one among all the possible energies $E_{\lambda,n}$. It is also numerically observed that $\langle x\rangle(t)$ is bounded by $a/2$ and $(\lambda - 1/2)a$: the particle, on average, never gets closer than $a/2$ to the reflecting walls at $x = 0$ and $x = \lambda a$. The product $\Delta x \Delta p$ is plotted as a function of time in figure 14.

Note that the inverse process—sudden compression of the well, $\lambda < 1$—is impossible: one cannot instantaneously generate a function vanishing for $\lambda a < x < a$ from a function

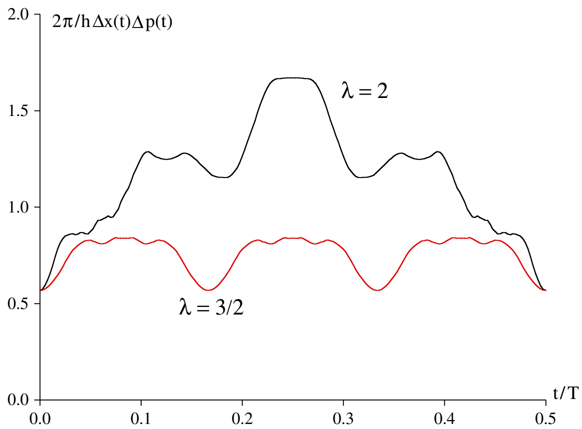

Figure 14. Variations in time ($0 \leqslant t \leqslant T/2$) of the product $\Delta x \Delta p$.

which is finite in that interval. An infinite well can only be compressed with a *finite* rate; this case was analysed in [22, 25].

As a final remark, let me mention that the limit $\lambda \to +\infty$ can be achieved from the above formula and indeed reproduces irreversible propagation in half-infinite space starting from the initial state $\psi_1(x)$; the point is to observe that $\Psi(x, t)$ in (2.4) is a summation on the variable $\nu = n/\lambda$, strictly equivalent to a Darboux sum, which quite naturally generates the Riemann integral over ν in this limit (the differential element dν arises spontaneously from the factor $1/\lambda$ in front of the summation). From (2.4), the limit $\lambda \to +\infty$ yields

$$\Psi(x, t) = \frac{\mathrm{i}\sqrt{2}}{a^{3/2}} \int_{-\infty}^{+\infty} \frac{\sin ka}{k^2 - (\pi/a)^2} \,\mathrm{e}^{\mathrm{i}kx}\, \mathrm{e}^{-\mathrm{i}\hbar k^2 t/(2m)} \mathrm{d}k. \tag{5.1}$$

Note that the two zeros of the denominator are just *apparent* singularities. Explicit direct calculation allows us to check that such an expression coincides with that obtained directly with the propagator of a free particle in $\mathbb{R}_+$:

$$U(x, t; x', 0) = \frac{2}{\pi} \int_0^{+\infty} \sin kx \sin kx' \,\mathrm{e}^{-\mathrm{i}\frac{\hbar k^2}{2m}t}\, \mathrm{d}k \quad (x, x' > 0) \tag{5.2}$$

acting on the initial state $\psi_1(x)$ to build the state at time t according to the standard way, $\Psi(x, t) = \int_{\mathbb{R}_+} U(x, t; x', 0)\Psi(x', 0)\mathrm{d}x'$. It is shown in appendix B that the expression (5.1) should not lead to misconceptions about the p-representation of this wave packet.

6. Concluding remarks

As stated from the beginning, this paper just aimed to present a brief review of the rather strange results given above. Although the general existence of the *plateaux* is numerically established, I was able up to this point to give only some elements of theoretical explanation and a genuine proof in the two particular cases $t = T/4, T/8$. Clearly, further investigation is required in order to provide a general demonstration and also to define a systematic method for finding the precise points (x_k, t_k) in spacetime where such intriguing behaviour takes place.

The fragmentation phenomenon also requires more attention although, as underlined, it is related to the well-known fractional revivals problem; at this point, it can be conjectured that for $t = T/2^{N+1}$ there exists a critical value $\lambda_c = 2^N$ above which spontaneous fragmentation occurs into 2^N peaks which are the translated *replica* of the initial density, divided by 2^N. I gave an analytical proof only for $N = 1, 2$, but numerical evidence allows us to be convinced that this is a general result. For $\lambda = \lambda_c$, the density is an ordered finite lattice of adjacent bumps. It cannot be excluded that more complex patterns could be realized, going beyond the simple organization observed for $t = T/2^{N+1}$, although numerical calculations for times of the form pT/M (p and M integers) have, until now, unveiled spatial organization having the simple features described above. Last but not least, a transparent physical interpretation would be welcome, allowing us to get physical insight explaining such amazing and counterintuitive behaviours. Work in these directions is in progress and, hopefully, will be published in the near future.

Finally, the relevance of the above results with regards to a given experiment is strongly dependent on the assumption of an *instantaneous* expansion of the well. Since the basic time scale is the period $T_1 = \frac{4ma^2}{\pi\hbar}$ defined in (1.2), it is hoped that the theoretical results should be observable provided the duration of the expansion is much smaller than T_1. For hydrogen (the lightest atom) initially confined in a well of nanoscale size ($a \sim 50$ Å), one has $T_1 \simeq 6 \times 10^{-10}$ s; with this, it can be hoped that a duration in the picosecond range at most should be adequate for the above results to be observed.

Acknowledgments

I am indebted to F Germain, D Mouhanna, J Vidal, J-M Maillard, O Bénichou and J M Raimond for helpful and fruitful discussions.

Appendix A

I here show how to check that the state $\Psi(x, t)$ given by equation (2.4) is actually normalized to unity and that the expectation value of the energy is indeed equal to E_1 for any time, as it must be on physical grounds since no work is done on the particle when the well is suddenly expanded.

Let us consider the function $G(\lambda, \phi)$ defined as follows (λ not an integer):

$$G(\lambda, \phi) = \sum_{n=-\infty}^{+\infty} \frac{\mathrm{e}^{2\mathrm{i}n\phi}}{\lambda^2 - n^2}; \tag{A.1}$$

this series is uniformly convergent for any real ϕ, so that $G(\phi)$ is a continuous function. On the other hand, derivatives of G obviously contain generalized functions (the unit-step function and its derivatives). One readily sees that the definition (A.1) allows us to write

$$|\langle\Psi(t)|\Psi(t)\rangle|^2 = -\frac{\lambda^2}{2\pi^2}\left(\frac{\partial}{\partial\lambda}[G(\lambda, 0) - G(\lambda, \phi)]\right)_{\phi=\pi/\lambda}. \tag{A.2}$$

Let us now find $G(\lambda, \phi)$, which is an even π-periodic function of the variable ϕ. By differentiating twice the definition (A.1), one obtains a linear combination of the function G itself and a Dirac comb. This means that the non-singular part of G precisely satisfies the differential equation $\partial_{\phi\phi}G + 4\lambda^2 G = 0$ for any $\phi \in]0, \pi/2[$; the general solution is $A\cos 2\lambda\phi + B\sin 2\lambda\phi$. The two constants A and B can be found by using the known equalities (Mittag–Leffler expansions):

$$G(\lambda, 0) \equiv \sum_{n=-\infty}^{+\infty} \frac{1}{\lambda^2 - n^2} = \frac{\pi}{\lambda}\cot\pi\lambda, \tag{A.3}$$

$$G(\lambda, \pi/2) \equiv \sum_{n=-\infty}^{+\infty} \frac{(-1)^n}{\lambda^2 - n^2} = \frac{\pi}{\lambda \sin \pi\lambda}, \tag{A.4}$$

which yield $A = \frac{\pi}{\lambda}\cot\lambda\pi$ and $B = \frac{\pi}{\lambda}$, so that eventually

$$G(\lambda, \phi) = \frac{\pi \cos\lambda(2|\phi| - \pi)}{\lambda \sin\pi\lambda} \quad (-\pi/2 \leqslant \phi \leqslant \pi/2). \tag{A.5}$$

As anticipated above, $G(\lambda, \phi)$ is a continuous function of ϕ, but its first derivative has a jump at $\phi = 0(\pi)$, explaining the presence of the Dirac comb in the complete second-order differential equation for $G(\lambda, \phi)$. Using now the rule expressed in (A.2), one readily gets $|\langle\Psi(t)|\Psi(t)\rangle|^2 = 1$.

As for the average of the energy, one has

$$\langle H\rangle = -\frac{\lambda E_1}{\pi^2}[G(\lambda, 0) - G(\lambda, \pi/\lambda)] - \frac{\lambda^2 E_1}{2\pi^2}\left(\frac{\partial}{\partial\lambda}[G(\lambda, 0) - G(\lambda, \phi)]\right)_{\phi=\pi/\lambda}; \tag{A.6}$$

the quantity in the brackets of the first line vanishes since it is proportional to $\Psi(x = a, 0)$; due to (A.2), one is eventually left with

$$\langle H\rangle = E_1|\langle\Psi(t)|\Psi(t)\rangle|^2 = E_1, \tag{A.7}$$

confirming that the expectation value of energy $\langle H\rangle$ is equal to E_1 at all times negative or positive, as it must be.

Appendix B

I here intend to draw attention on a misconception which could arise in view of the expression (5.1). In order to make the discussion easier, I rewrite the latter as follows:

$$\Psi(x, t) = \frac{1}{\sqrt{2\pi\hbar}} \int_{-\infty}^{+\infty} \mathrm{e}^{\mathrm{i}px/\hbar}\,\tilde{\Phi}(p)\,\mathrm{e}^{-\mathrm{i}p^2t/(2m\hbar)}\,\mathrm{d}p, \tag{B.1}$$

where the function $\tilde{\Phi}(p)$ is

$$\tilde{\Phi}(p) = \frac{2p_0^{3/2}}{\mathrm{i}\pi}\frac{\sin(\pi p/p_0)}{p_0^2 - p^2}, \qquad p_0 = \frac{\pi\hbar}{a}. \tag{B.2}$$

At first sight, it looks obvious to state that $\tilde{\Phi}(p)$ is the p-representation of the initial state, while the time-dependent exponential in the integral in (B.1) is just the ordinary phase factor for the free particle starting in the $\tilde{\Phi}(p)$ state at initial time. As apparently trivial as it stands, this statement is simply wrong. In order to show this, let us draw a few consequences of it.

First, it is easy to calculate the integral $\int_{-\infty}^{+\infty} |\tilde{\Phi}(p)|^2\,\mathrm{d}p$; one finds that it is equal to 2, instead of 1. Second, the true p-representation of the initial state can be easily and unambiguously calculated according to $\Phi(p, t = 0) = (\pi\hbar a)^{-1/2}\int_0^a \mathrm{e}^{-\mathrm{i}px/\hbar}\sin(\pi x/a)\mathrm{d}x$, and turns out to be

$$\Phi(p, 0) = \frac{1}{\pi}\frac{p_0^{3/2}}{p_0^2 - p^2}(1 + \mathrm{e}^{-\mathrm{i}\pi p/p_0}); \tag{B.3}$$

aside the fact that it comes out properly normalized to unity since $\Psi(x, 0)$ is, the function $\Phi(p, 0)$ is frankly different from the function $\tilde{\Phi}(p)$ given in (B.2). Another drawback is that, due to standard rules of quantum mechanics for p-representation, the expectation value of the coordinate is

$$\langle x\rangle(t) = \mathrm{i}\hbar \int_{-\infty}^{+\infty} \mathrm{d}p \tilde{\Phi}^*(p) \left[\frac{\mathrm{d}}{\mathrm{d}p} \tilde{\Phi}(p) - \frac{\mathrm{i}pt}{m\hbar} \tilde{\Phi}(p) \right]. \tag{B.4}$$

Since $\tilde{\Phi}(p)$ is an odd function of p, the integral vanishes, giving $\langle x\rangle(t) = 0$, which is clearly incorrect: the wave packet moves (and spreads out) in the free half-infinite space as time goes on. On the other hand, a non-vanishing integral would give a purely imaginary expectation value since $\tilde{\Phi}(p)$ is a real-valued function, up to a constant phase.

The error comes from the fact that everything stands in $\mathbb{R}_+$, instead of $\mathbb{R}$. In other words, when a function $f(x)$ arises as a Fourier integral of the form

$$f(x) = \frac{1}{\sqrt{2\pi}} \int_{-\infty}^{+\infty} \mathrm{e}^{\mathrm{i}kx} \tilde{F}(k)\, \mathrm{d}k, \tag{B.5}$$

the equality holds true only for $x > 0$ and one must not conclude at a glance (although this could happen to be correct) that the function $\tilde{F}(k)$ is the Fourier transform of $f(x)$: since all this holds true only if $x > 0$, and assuming that the Jordan's lemma is applicable, one can add to $\tilde{F}(k)$ any function $\phi(k)$ which is analytic in the complex upper half-plane without changing the integral on the RHS of (B.5); the difference between $\tilde{\Phi}(p)$ and $\Phi(p, 0)$ is actually such a function (remember that $\pm p_0$ are apparent singularities). In other words, although the Fourier transformation $f(x) \to F(k)$ is unambiguous, any intervening Fourier integral must be cautiously interpreted before to claim this is just the Fourier inversion formula; unconsidered intuitive identification can give incorrect results. Recall that for such functions defined in $\mathbb{R}_+$, the Laplace transformation is a much more secure method to proceed.

References

[1] Abramowitz M and Stegun I A 1972 *Handbook of Mathematical Functions* (New York: Dover) chapter 16
[2] Holschneider M 1988 On the Wavelet Transformation of Fractal Objects *J. Stat. Phys.* **50** 963
[3] Styer D F 2001 Quantum revivals versus classical periodicity in the infinite square well *Am. J. Phys.* **69** 56
[4] Eberly J H, Narozhny N B and Sanchez-Mondragon J J 1980 Periodic spontaneous collapse and revival in a simple quantum model *Phys. Rev. Lett.* **44** 1323
[5] Averbukh I Sh and Perelman N F 1991 The dynamics of wave packets of highly-excited atoms and molecules *Sov. Phys.—Usp.* **34** 572
[6] Leichtle C, Averbukh I Sh and Schleich W P 1996 Multilevel quantum beats *Phys. Rev.* A **54** 5299
[7] Robinett R W 2004 Quantum wave packets revivals *Phys. Rep.* **392** 1
[8] Aronstein D L and Stroud C R Jr 1997 Fractional wave-function revivals in the infinite square well *Phys. Rev.* A **55** 4526
[9] Chen Bing, Song Z and Sun C P 2007 Fractional revivals of the quantum state in a tight-binding chain *Phys. Rev.* A **75** 012113
[10] Bender C M, Brody D J and Meister B K 2005 Unusual quantum states: non-locality, entropy, Maxwell's demon and fractals *Proc. R. Soc.* **461** 733
[11] Berry M V 1996 Quantum fractals in boxes *J. Phys. A: Math. Gen.* **29** 6617
[12] Berry M V and Bodenschatz E 1999 Caustics, multiply-reconstructed by Talbot interference *J. Mod. Opt.* **46** 965
[13] Rojo A, Cohen J L and Berman P R 1999 Talbot oscillations and periodic focusing in a one-dimensional condensate *Phys. Rev.* A **60** 1482
[14] Campo A del and Muga J G 2006 Dynamics of a Tonks–Girardeau gas released from a hard-well trap *Europhys. Lett.* **74** 3493
[15] Hall M J W, Reineker M S and Schleich W P 1999 Unravelling quantum carpets: a travelling-wave approach *J. Phys. A: Math. Gen.* **32** 8275
[16] Appel W 2002 *Mathématiques pour la physique et les physiciens* (Paris: H & K Éditions)
[17] Aslangul Cl 1995 δ well with a reflecting barrier *Am. J. Phys.* **63** 935
[18] Corkum P B and Krausz F 2007 Attosecond science *Nature Phys.* **3** 381

[19] Corkum P B 1993 Plasma perspective on strong field multiphoton ionization *Phys. Rev. Lett.* **71** 1994
[20] Leweinstein M, Balcou P, Ivanov M Y, L'Huillier A and Corkum P B 1994 Theory of high-harmonic generation by low-frequency laser fields *Phys. Rev.* A **49** 2117
[21] Hall J L and Hänsch T W 1984 External dye-laser frequency stabilizer *Opt. Lett.* **9** 502
[22] Doescher S W and Rice M H 1969 Infinite Square-well potential with a moving wall *Am. J. Phys.* **37** 1246
[23] Schlitt D W and Stutz C 1970 An instructive example of the sudden-approximation in quantum mechanics *Am. J. Phys.* **38** 70
[24] Cordes J G, Kiang D and Nakajima H 1984 On the sudden expansion of an infinite square well *Am. J. Phys.* **52** 155
[25] Pinder D N 1990 The contracting square quantum well *Am. J. Phys.* **58** 54